Available online at www.sciencedirect.com
SCIENCE DIRECT®
Biochimica et Biophysica Acta 1655 (2004) 282–289
BIOCHIMICA ET BIOPHYSICA ACTA
BBA
www.bba-direct.com

Review

UV optical absorption by protein radicals in cytochrome *c* oxidase

Denis A. Proshlyakov*

Department of Biochemistry and Molecular Biology, Michigan State University, East Lansing, MI 48824, USA

Received 6 May 2003; accepted 23 October 2003

Abstract

The UV properties of key oxygen intermediates of cytochrome *c* oxidase have been investigated by transient absorption spectroscopy. The temporal behavior of $\mathbf{P_m}$ species upon aerobic incubation with CO or in the reaction with H_2O_2 is closely concurred by a new optical shift at 290/260 nm. In the acid-induced conversion of $\mathbf{P_m}$ to $\mathbf{F}^{\bullet}$, it is replaced by another shift at 323/288 nm. The wavelength and intensity of the UV signal observed in $\mathbf{F}^{\bullet}$ match closely the properties of model $\mathbf{Trp}^{\bullet}$ in agreement with results of ENDOR studies on this species. The UV spectrum of $\mathbf{Tyr}^{\bullet}$ gives the closest match with the 290/260 nm signal observed in $\mathbf{P_m}$. On the basis of analysis of possible UV chromophores in CcO and similarity to $\mathbf{Tyr}^{\bullet}$, the 290/260 nm signal is proposed to originate from the H^{240}-$Y^{244\bullet}$ site. Possible effects of local environment on UV properties of this site are discussed.

Keywords: Cytochrome oxidase; Reactive intermediate; Tyrosine radical; Tryptophan radical; Optical absorption

1. Introduction

The question as to how O_2 is reduced by the terminal enzyme of the mitochondrial respiratory chain, cytochrome *c* oxidase (CcO), has been a controversial issue over the past decade. While there has long been consensus about structures of most reactive intermediates [1,2], detailed structure of a $\mathbf{P_m}$[1] species remains an open question. Oxidation state of $\mathbf{P_m}$ corresponds to that of peroxide in the solution (hence "peroxy" or **P**), since it is produced when two electrons and O_2 react (either sequentially or as H_2O_2) with the oxidized enzyme [3–7]. Resonance Raman studies on $\mathbf{P_m}$ and successive **F** (or "ferryl") species showed that the O–O bond in $\mathbf{P_m}$ is already broken [5,8,9] and that this occurs immediately following transfer of the second electron to the primary Fe^{II}-O_2 species [7]. Release of one of the oxygen atoms from the active site, in the form of water, strongly supported this assignment [10]. Because metal centers in the binuclear center could supply only three e^- out of four e^- required for cleavage of the O–O bond, the existence of an additional redox center has been proposed [4,5,7,9,11].

In the absence of spectroscopic evidence for involvement of an additional electron donor, discovery of an unusual cross-link between H^{240} and Y^{244} (bovine nomenclature) hinted its identity [12–15]. By utilizing a selective reactivity of iodide with aromatic radicals, it became possible to show that the active site of $\mathbf{P_m}$ does, indeed, contain an extra oxidizing equivalent [16]. Amino acid sequencing of the labeled protein pinpointed its location to the H^{240}-Y^{244} dimer.

Spectroscopic detection of $Y^{244\bullet}$ remains elusive. A close proximity of putative radical site to nearby paramagnetic Cu_B, enhanced by the presence of covalent bridging, makes both centers invisible for traditional EPR spectroscopy [4,7,17]. While optical absorption by radicals [18–22] can be used for their detection in non-heme enzymes [23–26], intense and variable visible absorption by the heme [27] obscures this region in CcO.

Because of the critical role the H^{240}-Y^{244} site is expected to play in catalysis, a number of studies have

* 38 Chemistry Bldg., Michigan State University, East Lansing, MI 48824,USA. Tel.: +1-517-355-9715x260; fax: +1-517-353-1793.
E-mail address: denisp@cem.msu.edu (D.A. Proshlyakov).

[1] **Ox**, fast oxidized form of CcO; $\mathbf{P_m}$, peroxy species produced from $2e^-$ reduced (mixed-valence) CcO in the reaction with O_2; **F**, ferryl species produced upon $1e^-$ reduction of $\mathbf{P_m}$; **F**, species at the same oxidation level as $\mathbf{P_m}$, yet exhibits visible spectrum identical to **F**; Tyr, **Tyr**, **Trp**, **Trp**, ground and $1e^-$ oxidized radical states of tyrosine and tryptophan, respectively.

0005-2728/$ - see front matter © 2004 Elsevier B.V. All rights reserved.
doi:10.1016/j.bbabio.2003.10.014

been initiated to detect and characterize this site in CcO. Particular emphasis is placed on vibrational characterization of model compounds in either UV [28,29] or IR regions [30–32], as reviewed elsewhere in this issue. An earlier study suggested that formation of $\mathbf{P_m}$ can cause conformational changes detectable in the UV region and suggested involvement of Tyr and Trp residues [33]. This study explores UV optical properties of three semi-stable reactive intermediates—$\mathbf{P_m}$, $\mathbf{F^{\bullet}}$, and **F**—in a view of current knowledge about mechanisms of CcO catalysis.

2. Materials and methods

Beef heart CcO was purified, as described earlier [16]. Room-temperature optical absorption measurements were carried out using a Hewlett Packard spectrophotometer model 8453 (Agilent Technologies, USA). For the peroxide reaction, a small (~1/1000) volume of H_2O_2 stock was injected into sample of oxidized CcO, and optical changes were followed between 0.1 s and 10 min. $\mathbf{P_m}$ was generated by aerobic incubation of 2–5 μM enzyme with CO delivered either by bubbling for 1 min or injection of CO-saturated buffer. $\mathbf{F^{\bullet}}$ species was generated from $\mathbf{P_m}$ upon acid jump, as follows: $\mathbf{P_m}$ was generated by mixing of ~150 μM CcO sample at pH 8.5 with CO-saturated buffer without gas phase, using two microsyringes. High concentration of reactants and sub-stochiometric amount of CO ensured that formation of $\mathbf{P_m}$ proceeded rapidly until CO was exhausted. CO removal was completed by aerobic incubation of 20–30 μl of sample for several minutes, while stirred. Absence of CO was imperative for high yield of $\mathbf{F^{\bullet}}$ in the next step. A concentrated sample of $\mathbf{P_m}$, thus generated, was injected into large excess of buffer at pH 6.5 and rapidly mixed. To

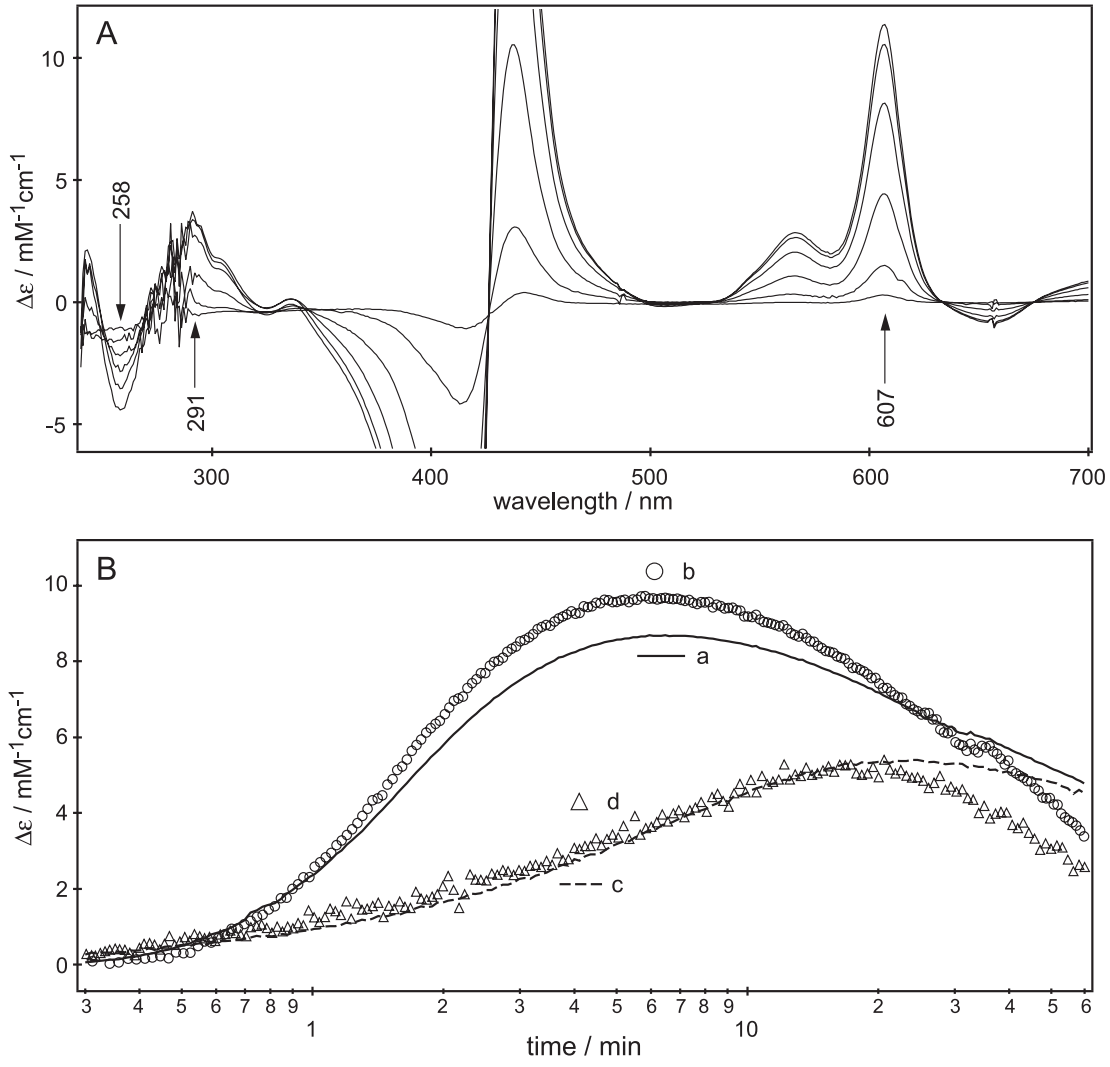

Fig. 1. Formation of $\mathbf{P_m}$ in aerobic reaction of oxidized CcO with CO. Panel A: UV–Vis difference absorption spectra observed at 48, 78, 110, 156, 231, and 333 s following bubbling of 5 μM CcO with CO for 60 s at pH 8.5. Panel B: Kinetics of optical changes observed at 607 nm (trace **a**) and difference $\Delta\varepsilon_{291} - \Delta\varepsilon_{258}$ (trace **b**) under conditions described for panel A. Traces **c** and **d**, respectively, were observed when CO-saturated buffer ($[CO]_{final} = 70$ μM) was added instead of bubbling.

account for spectral changes occurring primarily due to sample dilution and bulk changes upon lowering of pH, a parallel experiment was repeated using Ar instead of CO.

3. Results

3.1. P_m formation by $CO+O_2$

Fig. 1A shows optical changes observed upon incubation of oxidized CcO in the presence of both CO and O_2 [34]. Formation of a low-spin ferryloxo heme causes red shift of the Soret band that overwhelms the blue region. An increasing intensity of α-band at 607 nm is a characteristic signature of $\mathbf{P_m}$ formation. A new difference pattern is prominently seen in the UV region as a shift of a band from ~260 nm in resting enzyme to 290 nm in $\mathbf{P_m}$. Half-width of negative and positive bands are 14 and 19 nm, respectively. A shoulder at ~304 nm and a weak band at ~336 nm can be seen in $\mathbf{P_m}$. Isosbestic points at 249, 270, and 341 nm indicate that a single process contributes to observed UV changes, and no side reactions occur on the time scale of minutes.

To examine if a 290/260 nm band arises from $\mathbf{P_m}$ or a separate species, temporal changes at 607 and 290/260 nm are compared in Fig. 1B. It was found that the

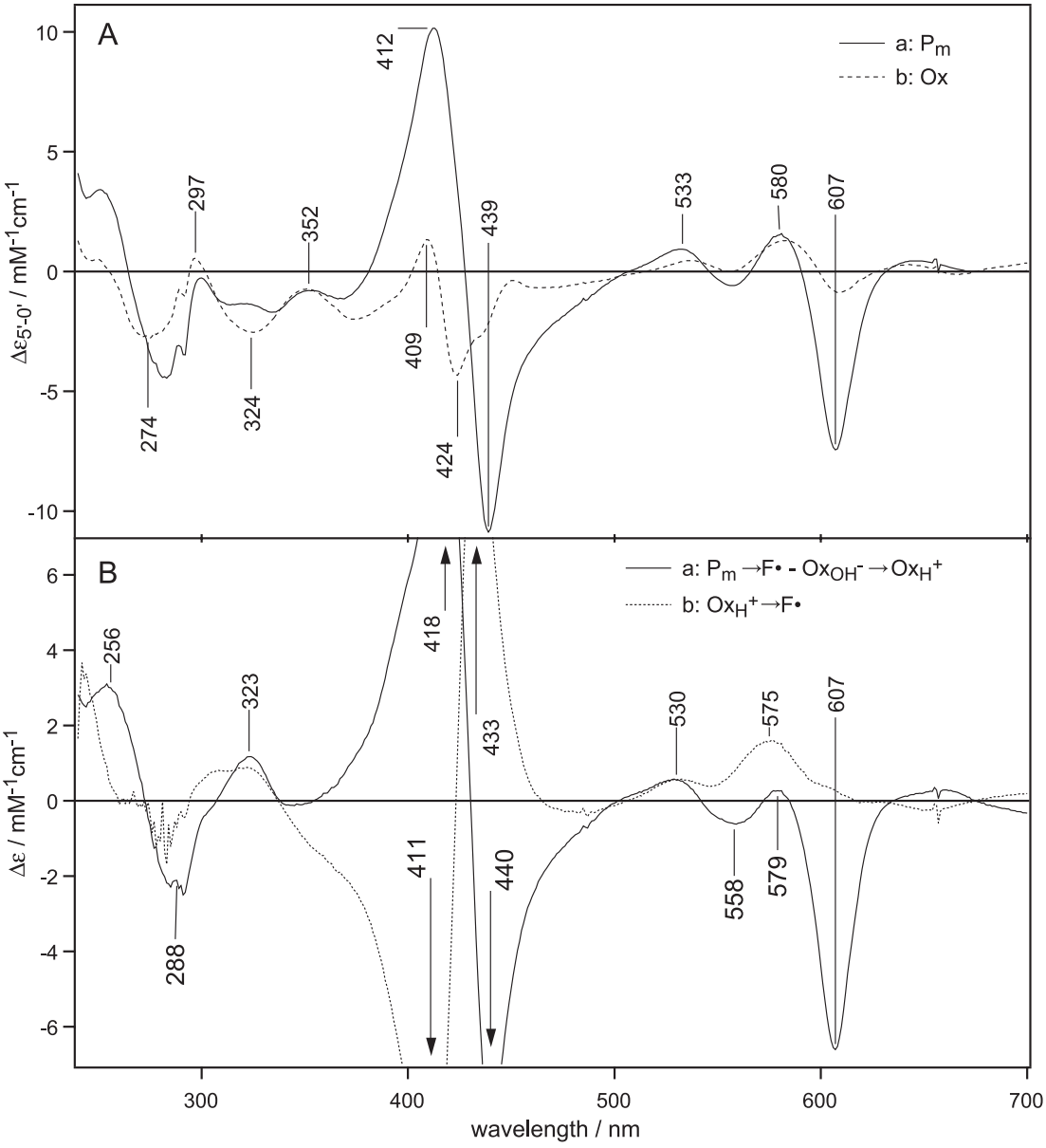

Fig. 2. Acid-induced optical changes in $\mathbf{P_m}$ and **Ox**. Panel A: Optical changes observed for $\mathbf{P_m}$ (a) and oxidized (Ar-treated) CcO (b) at 5 min following pH jump from 8.5 to 6.5. Panel B: Trace **a**, spectrum of $\mathbf{P_m}\rightarrow\mathbf{F^\bullet}$ transition obtained as a difference of traces **a** and **b** in panel A; trace **b**, difference spectrum of $\mathbf{F^\bullet}$ versus oxidized CcO obtained by subtracting contribution of $\mathbf{P_m}$ from trace **a**, as described in text.

behavior of the 290/260 band over the first ~20 min at room temperature does, indeed, concur with that of the 607-nm band. This was also the case when the rate of $\mathbf{P_m}$ formation was varied due to concentration of CO in the solution. Additional process begins to contribute in the UV region at later times and most likely is associated with stability of the enzyme, since it did not depend on initial kinetics.

3.2. Peroxide reaction

UV optical properties of $\mathbf{P_m}$ and **F** in the peroxide reaction were reexamined in time-resolved measurements using concentrations of H_2O_2 of 0.5 to 10 mM, i.e. $\times 100$ higher than that in the previous study [33]. Optical changes around 280 nm were identical to those observed in the $CO + O_2$ reaction and closely followed evolution of $\mathbf{P_m}$ (not shown). No lag was detected between development of $\mathbf{P_m}$ and the UV shift, even at highest concentrations of H_2O_2. This contradicts the previous assignment of the 280-nm shift to conformational changes at Cu_B site prior to $\mathbf{P_m}$ formation [33], as such two phases would be better resolved at high reaction rates. No UV signals were detected in **F**, except for gradual background changes, presumably due to structural damage.

3.3. pH-induced $P_m \rightarrow F^{\bullet}$ transition

Fig. 2A compares spectral changes in the oxidized enzyme and $\mathbf{P_m}$ over the first 5 min following change of pH from 8.5 to 6.5. Conversion of $\mathbf{P_m}$ in to $\mathbf{F^{\bullet}}$ is evident from loss of intensity at 607 nm with concurrent increase at 580 and 530 nm (trace **a**) [35]. Comparison between CO- (trace **a**) and Ar-treated (trace **b**) samples shows that the $\mathbf{P_m} \rightarrow \mathbf{F^{\bullet}}$ transition involves significant changes in the UV region, in addition to background changes observable with **Ox**. Trace **a** in Fig. 2B shows difference between traces **a** and **b** in Fig. 2A and corresponds to isolated contribution of $\mathbf{P_m} \rightarrow \mathbf{F^{\bullet}}$ transition. This double difference spectrum can be presented as $(\mathbf{F}^{\bullet}_{acid} - \mathbf{Ox}_{acid}) - (\mathbf{P_m}_{\ base} - \mathbf{Ox}_{base})$, where the latter term corresponds to formation of $\mathbf{P_m}$ at high pH. Hence, difference spectrum of $\mathbf{F^{\bullet}}$ formation at acidic pH can be isolated by subtracting spectrum of $\mathbf{Ox} \rightarrow \mathbf{P_m}$ transition (Fig. 1A), as shown by trace **b**. To account for partial completion of $\mathbf{P_m} \rightarrow \mathbf{F^{\bullet}}$ transition and decay of both species, spectrum of $\mathbf{P_m}$ from Fig. 1 was reduced upon subtraction so that the resulting spectrum did not exhibit significant 607-nm peak. The red region of trace **b** (Fig. 2B) closely matches experimental spectrum of $\mathbf{F/F^{\bullet}}$ formed by H_2O_2 at acidic pH, while UV region exhibits a single shift from ~282 to 322 nm.

Changes observable in the control (Ar-treated) enzyme are likely to be due to global conformational changes upon pH transition. The 324- and 352-nm bands appear in the region free from protein absorption and should be attributed to hemes and/or Cu_B. Although the 274 and 297 nm bands appear close to the protein 280-nm band, direction of an apparent shift is opposite to what would be expected if it arose from protonation of **Tyr**. Several heme transitions and charge-transfer (CT) bands of Cu^{2+}-OH^- and Cu^{2+}-imidazole are expected in this region (see below).

4. Discussion

$\mathbf{P_m}$ and $\mathbf{F^{\bullet}}$ are the two primary species in the peroxide reaction at high and low pH, respectively [35,36]. Both species have ferryloxo structure of heme a_3 and contain additional oxidizing equivalent at the active site. Radioactive labeling showed that Y^{244} in $\mathbf{P_m}$ is oxidized [16]. Recent ENDOR studies on $\mathbf{F^{\bullet}}$ revealed an unusual radical signal similar to the spectrum of $W^{191\bullet}$ in cytochrome *c* peroxidase compound ES [37,38]. At the same time, $\mathbf{P_m}$ and $\mathbf{F^{\bullet}}$ exhibit distinct and characteristic changes in the UV region, as shown here. These changes disappear upon reduction into subsequent **F** species. This is the most striking in $\mathbf{F^{\bullet}}$, which is spectrally indistinguishable from **F** above 400 nm [35]. It is therefore tempting to correlate observed UV changes with these additional redox centers. However, because CcO contains multiple redox cofactors and $\mathbf{P_m}$ lacks a good reference species (like $\mathbf{F/F^{\bullet}}$), several possible origins must be considered before conclusive assignment can be made.

4.1. Heme a_3

$\mathbf{P_m}$ and **F** species exhibit surprisingly large spectral difference in the red region. While possible causes for this have been discussed [7,39], it is not known how much the same factors could affect the UV region of the spectrum. Knowledge of UV properties of hemes below 300 nm is mostly derived from computational studies, which predicted a number of high-energy $\pi-\pi^*$ transitions sensitive to oxidation state and axial ligands [40–43]. Intensities of these transitions rely on dipole transition moments of isolated pyrrole rings and, therefore, are significantly weaker than that of B and Q bands that rely on the entire macrocycle [43]. As a result, N and L bands between 300 and 360 nm are typically the highest-energy transitions experimentally observable in heme proteins [44,45] and could contribute to the spectral changes shown in Fig. 2A. The next high-energy transition observed for model porphyrin complexes in gas phase is the M band around 225 nm [43,46] leaving a gap in the 240–300-nm region. Consistently, **F** and **Ox** show little difference in this region, suggesting that the signal observed in $\mathbf{P_m}$ is not likely to be significantly contributed by the heme.

4.2. Cu_B

Geometry and electronic configuration of Cu_B in each particular species will have strong influence on its UV

spectrum[47]. While it is conceivable that the extra oxidizing equivalent in $\mathbf{P_m}$ is located on Cu_B instead of Y^{244}, stable Cu^{3+} is unprecedented in biology [48], suggesting a Cu_B^{2+} state in all ferryl species. Geometry of its three His ligands does not change significantly in different redox states [13,49]. Binding of H_2O/OH^- at the forth position upon O–O bond cleavage [7,50] will produce distorted tetrahedral Cu^{2+} configuration that is likely to occur in all species discussed here. UV properties of such configuration are mostly defined by ligand-to-metal CT transitions, i.e. from ligand valence orbitals into Cu^{2+} d_{x2-y2} orbital. Particularly relevant OH → Cu and Im → Cu CT transitions appear around 300 nm with significant intensity [51–53]. While there is currently no evidence to suggest that significant changes in the geometry of Cu_B alone occur between $\mathbf{P_m}$ and **F** species, Cu_B is likely to play a significant role in the UV properties of CcO, especially in interactions with H^{240}-Y^{244} site (see below).

4.3. Protein moiety

In addition to **Tyr**, **Trp**, and **Phe**, UV optical absorption by CcO is contributed by the H^{240}-Y^{244} chromophore [12–15]. While changes in the oxidation state, geometry, or local charges of either of these centers could alter their spectra, the range of transitions that can *realistically* occur in proteins is very limited.

Theoretical studies showed that **Tyr** and **Trp** are fairly robust chromophores [54], not readily susceptible to conformational changes, especially in a rigid protein environment. Effect of local interactions on the electronic spectrum of **Tyr** is limited to hydrogen bonding to the phenol OH group [54]. Because of an energetic penalty for uncompensated charges in a low dielectric environment, deprotonation of a strong base must be coupled to significant electrostatic and/or redox changes [55,56]. Energy of such interaction(s) necessary to deprotonate Tyr ($pK = 10.5$) at pH = 7 should be ~200 mV. Corresponding energy for Trp ($pK = 16.9$ [57]) is ~600 mV, while Phe does not have dissociable protons. This shows that spectra of any of the aromatic residues are not likely to be affected by conformational changes in protein environment, as suggested previously [33].

Electronic absorption by aromatic residues is significantly affected by oxidation. **Tyr**, **Trp**, and a model for H^{240}-Y^{244} cross-linked site, **Im♦CrOH** [29,30,58], all have relatively low oxidation potential, especially when coupled to a loss of proton [56]. Catalytic radicals of both **Tyr** and **Trp** are well documented in a variety of enzymes [59,60]. Transient studies on **Tyr** and **Trp** radicals revealed characteristic signatures in the visible spectra and hinted even stronger changes in the UV region [18–21]. Maximal absorption by $\mathbf{Phe}^{+\bullet}$ appears at ~250 nm [22] similar to the phenyl radical [61,62] and much higher energy than the signal observed for CcO. Furthermore, oxidation of **Phe** is unlikely because of its high oxidation potential. This reduces the range of possible transitions involving aromatic residues to oxidation and/or (de)protonation of **Tyr** and **Trp** residues.

4.3.1. Origin of UV signal in $F^{\bullet}$

Currently, $\mathbf{F}^{\bullet}$ cannot be generated directly without a host of side reactions involving H_2O_2 [63], including formation of noncatalytic radicals that will contribute to the UV region [37,64–68]. Consequently, in this study, $\mathbf{F}^{\bullet}$ was generated indirectly from $\mathbf{P_m}$ species by lowering the pH of the sample [35]. Spectral similarity between $\mathbf{F}^{\bullet}$ and **F** in the visible region strongly suggests that the observed 322/282 nm shift does not originate from either of the two hemes. The wavelength of the positive band at 322 nm, however, is close to the reported absorption maximum of the of **Trp** radical species [21]. While no difference spectra of **Trp** oxidation were reported below 300 nm, the negative component at 282 nm is very close to absorption maximum of ground state **Trp**. The yield of calculated $\mathbf{F}^{\bullet}$ species in trace **b** (Fig. 2B) is approximately 40%, if extinction of 5.5 mM^{-1} cm^{-1} is assumed for the 575-nm peak [69]. When this spectrum was scaled to 100% occupancy at 575 nm, the amplitude of the 322-nm band was close to that of transient $\mathbf{Trp}^{\bullet}$ [21]. Thus, there is a good match between the 322/282-nm shift and expected difference spectrum of oxidation of **Trp**. The wavelength and the intensity of the positive band, however, appear closer to those of neutral $\mathbf{Trp}^{\bullet}$ rather than cation $\mathbf{TrpH}^{+\bullet}$, while ENDOR analysis by Rich and coworkers favored the cation species [37,38]. Published optical spectra of $\mathbf{Trp}^{\bullet}$ and $\mathbf{TrpH}^{+\bullet}$ in the UV region do not allow to identify, conclusively, which form is present in CcO, but both spectroscopic techniques are in agreement about the oxidation of **Trp** residues.

4.3.2. Origin of UV signal in P_m

Tyr and its specific derivative **Im♦CrOH** have sufficiently low oxidation potential and low pK_a of phenol oxygen, so that either oxidation or deprotonation (see above) can occur. Optical shift of approximately 306/280 nm associated with deprotonation of **Im♦CrOH** can be deduced from published data [29,30] and is ~20 nm to red from the signal in $\mathbf{P_m}$. While optical changes associated with oxidation of **Im♦CrOH** are not known, to some extent they can be anticipated. Transient UV spectrum of $\mathbf{TyrO}^{\bullet}$, reported previously, suggests significant perturbations of the 200–300-nm region upon oxidation, although it is not possible to calculate a reliable difference spectrum needed for comparison with CcO. Such difference spectrum was obtained experimentally and shown in Fig. 3. It can be seen in Fig. 3 that $\mathbf{TyrO}^{-} \rightarrow \mathbf{TyrO}^{\bullet}$ transition is associated with the optical shift from 235 to 268 nm, while the visible region shows formation of a characteristic band at 410 nm. Since pK_a of $\mathbf{TyrO}^{\bullet}$ is as low as −2 [20,70], its spectrum will show little pH sensitivity, and a shift from ~220 to ~270 nm can therefore be estimated for the

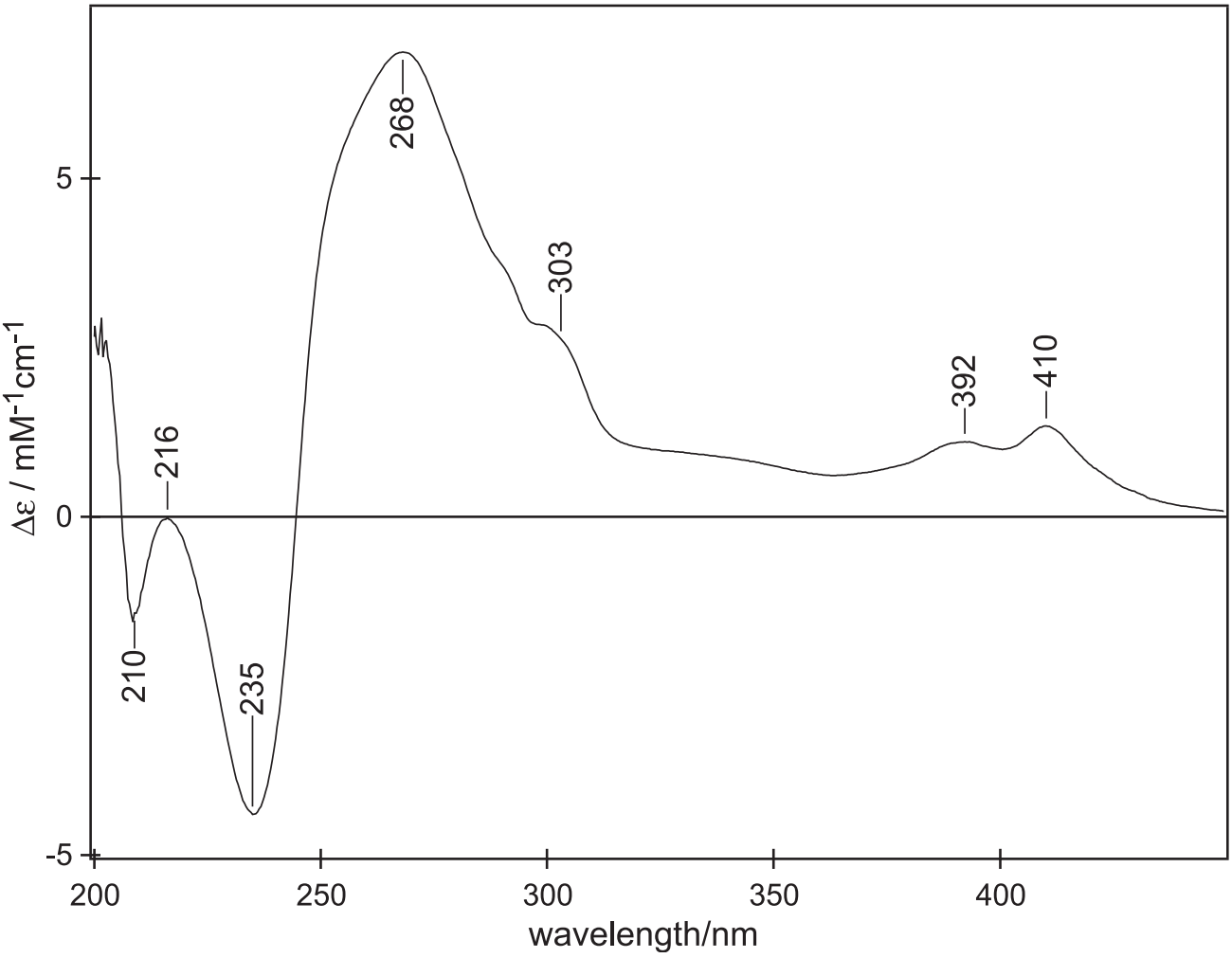

Fig. 3. UV difference absorption spectrum of oxidation of Tyr. Glassy samples of 250 μM Tyr in 5 mM LiOH, 7 M LiCl, were oxidized at 140 K by UV output of Hg arc lamp. The spectrum shown was obtained by global exponential fitting of ~100 spectra acquired between 0.1 s and 60 min of illumination.

TyrOH → **TyrO**$^{\bullet}$ transition. In either case, oxidation of **Tyr** produces optical changes that are closest among aromatic amino acids to that observed in $\mathbf{P_m}$. Amplitudes of signals observed for **Tyr** and CcO of ~10 mM^{-1} cm^{-1} are in good agreement as well.

The apparent 23-nm difference between UV shift of **TyrO**$^{\bullet}$ and $\mathbf{P_m}$ may be accounted for by the presence of the covalent bond between Y^{244} and H^{240} and their binding to Cu_B. The electrostatic effect of a partial atomic charge of imidazole nitrogen near the ortho-carbon of phenol is similar to the effect of hydrogen bonding and deprotonation of phenol hydroxy group in the solution [54]. In fact, all reported spectra of models of the H^{240}-Y^{244} site consistently show ~10-nm red shift of the phenol ring π–π* transitions from that of **Tyr**, compared to 19-nm red shift upon deprotonation of either compound [29,30,58]. Mixing of π-orbitals at small dihedral angles between imidazole and phenol rings, like in CcO [13], will create a longer conjugated orbital, causing further red shift. A small shift in absorption of phenol moiety in response to protonation of imidazole nitrogen, significant increase in acidity of both moieties, as well as change in the acidity of imidazole upon oxidation of phenol all indicate that such electronic interactions take place [29,30,58]. Lastly, binding to Cu_B is likely to alter the electronic configuration of imidazole/phenol π-coupled dimer, as well as conjugation with Y^{244} will necessarily affect H^{240}→Cu ligand-to-metal CT bands, which are expected in the 300-nm region. Delocalization of the radical between imidazole and phenol creates a possibility of a metal-to-ligand CT transition, which will be equivalent to a transient formation of a Cu^{3+}-HY^{-} state. Intricate details of the H^{240}-Y^{244}-Cu_B site are beginning to be addressed, as more sophisticated, second-generation models become available [71,72].

The analysis presented here demonstrates that biological radicals, such as **Tyr**$^{\bullet}$ and **Trp**$^{\bullet}$, can be detected and identified by their UV absorption properties even in such complex systems as CcO. This is illustrated by detection of **Trp**$^{\bullet}$ in **F**$^{\bullet}$. Spectrum of **Tyr**$^{\bullet}$ is the closest to the signal observed in $\mathbf{P_m}$, although no exact match was identified. This signal is proposed to arise from oxidation of Y^{244} with altered UV properties due to cross-linking to Cu_B-bound H^{240}.

Efforts are currently under way to test this assignment by characterizing the UV absorption properties of corresponding model radicals.

Acknowledgements

This work was initiated under the guidance of Gerald T. Babcock—an outstanding and generous colleague, who is greatly missed. The author thanks Dr. Shelagh Ferguson-Miller, Dr. Warwick Hillier and all members of Babcock's group for helpful discussions. This work was supported by NIH GM25480 and GM37300 grants.

References

[1] S. Ferguson-Miller, G.T. Babcock, Heme/copper terminal oxidases, Chem. Rev. 96 (1996) 2889–2907.
[2] T. Kitagawa, Structures of reaction intermediates of bovine cytochrome *c* oxidase probed by time-resolved vibrational spectroscopy, J. Inorg. Biochem. 82 (2000) 9–18.
[3] B. Chance, C. Saronio, J.S. Leigh, Compound-C_2, a product of the reaction of oxygen and the mixed-valence state of cytochrome-oxidase—optical evidence for a type-I copper, Biochem. J. 177 (1979) 931–941.
[4] L.C. Weng, G.M. Baker, Reaction of hydrogen-peroxide with the rapid form of resting cytochrome-oxidase, Biochemistry-Us 30 (1991) 5727–5733.
[5] D.A. Proshlyakov, T. Ogura, K. Shinzawaitoh, S. Yoshikawa, E.H. Appelman, T. Kitagawa, Selective resonance Raman observation of the 607 nm form generated in the reaction of oxidized cytochrome *c* oxidase with hydrogen-peroxide, J. Biol. Chem. 269 (1994) 29385–29388.
[6] M. Fabian, G. Palmer, The reaction of cyanide with peroxidatic forms of cytochrome-oxidase, Biochemistry-Us 34 (1995) 1534–1540.
[7] D.A. Proshlyakov, M.A. Pressler, G.T. Babcock, Dioxygen activation and bond cleavage by mixed-valence cytochrome *c* oxidase, Proc. Natl. Acad. Sci. U. S. A. 95 (1998) 8020–8025.
[8] D.A. Proshlyakov, T. Ogura, K. ShinzawaItoh, S. Yoshikawa, T. Kitagawa, Resonance Raman/absorption characterization of the oxo intermediates of cytochrome *c* oxidase generated in its reaction with hydrogen peroxide: pH and H_2O_2 concentration dependence, Biochemistry-Us 35 (1996) 8580–8586.
[9] D.A. Proshlyakov, T. Ogura, K. ShinzawaItoh, S. Yoshikawa, T. Kitagawa, Microcirculating system for simultaneous determination of Raman and absorption spectra of enzymatic reaction intermediates and its application to the reaction of cytochrome *c* oxidase with hydrogen peroxide, Biochemistry-Us 35 (1996) 76–82.
[10] M. Fabian, W.W. Wong, R.B. Gennis, G. Palmer, Mass spectrometric determination of dioxygen bond splitting in the "peroxy" intermediate of cytochrome *c* oxidase, Proc. Natl. Acad. Sci. U. S. A. 96 (1999) 13114–13117.
[11] C.W. Hoganson, M.A. Pressler, D.A. Proshlyakov, G.T. Babcock, From water to oxygen and back again: mechanistic similarities in the enzymatic redox conversions between water and dioxygen, Biochim. Biophys. Acta 1365 (1998) 170–174.
[12] C. Ostermeier, A. Harrenga, U. Ermler, H. Michel, Structure at 2.7 angstrom resolution of the *Paracoccus denitrificans* two-subunit cytochrome *c* oxidase complexed with an antibody F-V fragment, Proc. Natl. Acad. Sci. U. S. A. 94 (1997) 10547–10553.
[13] S. Yoshikawa, K. Shinzawa-Itoh, R. Nakashima, R. Yaono, E. Yamashita, N. Inoue, M. Yao, M.J. Fei, C.P. Libeu, T. Mizushima, H. Yamaguchi, T. Tomizaki, T. Tsukihara, Redox-coupled crystal structural changes in bovine heart cytochrome *c* oxidase, Science 280 (1998) 1723–1729.
[14] R.B. Gennis, Multiple proton-conducting pathways in cytochrome oxidase and a proposed role for the active-site tyrosine, Biochim. Biophys. Acta 1365 (1998) 241–248.
[15] G. Buse, T. Soulimane, M. Dewor, H.E. Meyer, M. Bluggel, Evidence for a copper-coordinated histidine-tyrosine cross-link in the active site of cytochrome oxidase, Protein Sci. 8 (1999) 985–990.
[16] D.A. Proshlyakov, M.A. Pressler, C. DeMaso, J.F. Leykam, D.L. DeWitt, G.T. Babcock, Oxygen activation and reduction in respiration: involvement of redox-active tyrosine 244, Science 290 (2000) 1588–1591.
[17] J.E. Morgan, M.I. Verkhovsky, G. Palmer, M. Wikstrom, Role of the P-R intermediate in the reaction of cytochrome *c* oxidase with O_2, Biochemistry-Us 40 (2001) 6882–6892.
[18] J. Feitelson, E. Hayon, Electron ejection and electron capture by phenolic compounds, J. Phys. Chem.-Us 77 (1973) 10–15.
[19] D.V. Bent, E. Hayon, Excited state chemistry of aromatic amino acids and related peptides: I. Tyrosine, J. Am. Chem. Soc. 97 (1975) 2599–2606.
[20] D.V. Bent, E. Hayon, Excited state chemistry of aromatic amino acids and related peptides: III. Tryptophan, J. Am. Chem. Soc. 97 (1975) 2612–2619.
[21] S. Solar, N. Getoff, P.S. Surdhar, D.A. Armstrong, A. Singh, Oxidation of tryptophan and *N*-methylindole by N_3^-, Br_2^-, and $(Scn)_2^-$ radicals in light-water and heavy-water solutions—a pulse-radiolysis study, J. Phys. Chem.-Us 95 (1991) 3639–3643.
[22] D.V. Bent, E. Hayon, Excited state chemistry of aromatic amino acids and related compounds: II. Phenylalanine, J. Am. Chem. Soc. 97 (1975) 2606–2612.
[23] L. Petersson, A. Graslund, A. Ehrenberg, B.M. Sjoberg, P. Reichard, The iron center in ribonucleotide reductase from *Escherichia coli*, J. Biol. Chem. 255 (1980) 6706–6712.
[24] C. Aubert, P. Mathis, A.P.M. Eker, K. Brettel, Intraprotein electron transfer between tyrosine and tryptophan in DNA photolyase from *Anacystis nidulans*, Proc. Natl. Acad. Sci. U. S. A. 96 (1999) 5423–5427.
[25] J. Baldwin, C. Krebs, B.A. Ley, D.E. Edmondson, B.H. Huynh, J.H. Bollinger, Mechanism of rapid electron transfer during oxygen activation in the R2 subunit of *Escherichia coli* ribonucleotide reductase: 1. Evidence for a transient tryptophan radical, J. Am. Chem. Soc. 122 (2000) 12195–12206.
[26] M.J. Ryle, A. Liu, R.B. Muthukumaran, R.Y.N. Ho, K.D. Koehntop, J. McCracken, L. Que, R.P. Hausinger, O_2- and alpha-ketoglutarate-dependent tyrosyl radical formation in TauD, an alpha-keto acid-dependent non-heme iron dioxygenase, Biochemistry-Us 42 (2003) 1854–1862.
[27] W.H. Vanneste, The stochiometry and absorption spectra of components *a* and a_3 in cytochrome *c* oxidase, Biochemistry-Us 5 (1966) 838–848.
[28] M. Aki, T. Ogura, K. Shinzawa-Itoh, S. Yoshikawa, T. Kitagawa, A new measurement system for UV resonance Raman spectra of large proteins and its application to cytochrome *c* oxidase, J. Phys. Chem., B 104 (2000) 10765–10774.
[29] M. Aki, T. Ogura, Y. Naruta, T.H. Le, T. Sato, T. Kitagawa, UV resonance Raman characterization of model compounds of Tyr(244) of bovine cytochrome *c* oxidase in its neutral, deprotonated anionic, and deprotonated neutral radical forms: effects of covalent binding between tyrosine and histidine, J. Phys. Chem., A 106 (2002) 3436–3444.
[30] J.A. Cappuccio, I. Ayala, G.I. Elliott, I. Szundi, J. Lewis, J.P. Konopelski, B.A. Barry, O. Einarsdottir, Modeling the active site of cytochrorne oxidase: synthesis and characterization of a cross-linked histidine-phenol, J. Am. Chem. Soc. 124 (2002) 1750–1760.
[31] F. Tomson, J.A. Bailey, R.B. Gennis, C.J. Unkefer, Z.H. Li, L.A. Silks, R.A. Martinez, R.J. Donohoe, R.B. Dyer, W.H. Woodruff, Di-

rect infrared detection of the covalently ring linked His-Tyr structure in the active site of the heme-copper oxidases, Biochemistry-Us 41 (2002) 14383–14390.
[32] M. Iwaki, J. Breton, P.R. Rich, ATR-FTIR difference spectroscopy of the P-M intermediate of bovine cytochrome *c* oxidase, Biochim. Biophys. Acta 1555 (2002) 116–121.
[33] R.W. Larsen, Peroxide-induced spectral perturbations of the 280-nm absorption band of cytochrome-*c*-oxidase, FEBS Lett. 352 (1994) 365–368.
[34] P. Nicholls, G.A. Chanady, Interactions of cytochrome-aa_3 with oxygen and carbon-monoxide—the role of the 607-nm complex, Biochim. Biophys. Acta 634 (1981) 256–265.
[35] M. Fabian, G. Palmer, Proton involvement in the transition from the "peroxy" to the ferryl intermediate of cytochrome *c* oxidase, Biochemistry-Us 40 (2001) 1867–1874.
[36] S. Junemann, P. Heathcote, P.R. Rich, The reactions of hydrogen peroxide with bovine cytochrome *c* oxidase, Biochim. Biophys. Acta 1456 (2000) 56–66.
[37] P.R. Rich, S.E.J. Rigby, P. Heathcote, Radicals associated with the catalytic intermediates of bovine cytochrome *c* oxidase, Biochim. Biophys. Acta 1554 (2002) 137–146.
[38] S.E.J. Rigby, S. Junemann, P.R. Rich, P. Heathcote, Reaction of bovine cytochrome *c* oxidase with hydrogen peroxide produces a tryptophan cation radical and a porphyrin cation radical, Biochemistry-Us 39 (2000) 5921–5928.
[39] M. Wikstrom, Mechanism of proton translocation by cytochrome *c* oxidase: a new four-stroke histidine cycle, Biochim. Biophys. Acta 1458 (2000) 188–198.
[40] P. Du, F.U. Axe, G.H. Loew, S. Canuto, M.C. Zerner, Theoretical-study on the electronic-spectra of model compound-II complexes of peroxidases, J. Am. Chem. Soc. 113 (1991) 8614–8621.
[41] D.L. Harris, G.H. Loew, Proximal ligand effects on electronic structure and spectra of compound I of peroxidases, J. Porphyr. Phthalocyanines 5 (2001) 334–344.
[42] K.M.T. Oliveira, M. Trsic, Comparative theoretical study of the electronic structures and electronic spectra of Fe2+-, Fe3+-porphyrin and free base porphyrin, J. Mol. Struct. Theochem 539 (2001) 107–117.
[43] E.J. Baerends, G. Ricciardi, A. Rosa, S.J.A. van Gisbergen, A DFT/TDDFT interpretation of the ground and excited states of porphyrin and porphyrazine complexes, Coord. Chem. Rev. 230 (2002) 5–27.
[44] M.W. Makinen, A.K. Churg, Structural and analytical aspects of the electronic spectra of hemeproteins, in: A.B.P. Lever, H.B. Gray (Eds.), Iron Porphyrins, Addison-Wesley Publishing, Reading, MA, 1983, pp. 141–235.
[45] W.A. Eaton, J. Hofrichter, Polarized absorption and linear dichroism spectroscopy of hemoglobin, in: N. Kaplan, N. Colowick (Eds.), Hemoglobins, Academic Press, New York, 1981, pp. 175–261.
[46] L. Edwards, D.H. Dolphin, M. Gouterman, Porphyrins: XVI. Vapor absorption spectra and redox reactions: octalkylporphyrins, J. Mol. Spectrosc. 35 (1970) 90–109.
[47] E.I. Solomon, M.D. Lowery, L.B. Lacroix, D.E. Root, Electronic absorption-spectroscopy of copper proteins, Methods Enzymol. 226 (1993) 1–33.
[48] K.D. Karlin, Z. Tyeklar, Bioinorganic Chemistry of Copper, Chapman & Hall, New York, 1993.
[49] A. Harrenga, H. Michel, The cytochrome *c* oxidase from *Paracoccus denitrificans* does not change the metal center ligation upon reduction, J. Biol. Chem. 274 (1999) 33296–33299.
[50] M.R.A. Blomberg, P.E.M. Siegbahn, G.T. Babcock, M. Wikstrom, Modeling cytochrome oxidase: a quantum chemical study of the O–O bond cleavage mechanism, J. Am. Chem. Soc. 122 (2000) 12848–12858.
[51] E. Bernarducci, P.K. Bharadwaj, K. Kroghjespersen, J.A. Potenza, H.J. Schugar, Electronic-structure of alkylated imidazoles and electronic-spectra of Tetrakis(Imidazole)Copper(II) complexes—molecular-structure of Tetrakis(1,4,5-Trimethylimidazole)Copper(II) diperchlorate, J. Am. Chem. Soc. 105 (1983) 3860–3866.
[52] T.G. Fawcett, E.E. Bernarducci, K. Kroghjespersen, H.J. Schugar, Charge-transfer absorptions of Cu(II)-Imidazole and Cu(II)-Imidazolate chromophores, J. Am. Chem. Soc. 102 (1980) 2598–2604.
[53] E. Prenesti, S. Berto, P.G. Daniele, Ultraviolet spectrophotometric characterization of copper(II) complexes with imidazole *N*-methyl derivatives of L-histidine in aqueous solution, Spectrochim. Acta, A Mol. Spectrosc. 59 (2003) 201–207.
[54] A. Smolyar, C.F. Wong, Theoretical studies of the spectroscopic properties of tryptamine, tryptophan and tyrosine, J. Mol. Struct., Theochem 488 (1999) 51–67.
[55] P.R. Rich, B. Meunier, R. Mitchell, A.J. Moody, Coupling of charge and proton movement in cytochrome *c* oxidase, Biochim. Biophys. Acta 1275 (1996) 91–95.
[56] C. Tommos, G.T. Babcock, Proton and hydrogen currents in photosynthetic water oxidation, Biochim. Biophys. Acta 1458 (2000) 199–219.
[57] G.D. Fasman (Ed.), Handbook of Biochemistry and Molecular Biology, 3rd ed., vol. 1, CRC Press, Cleveland, OH, 1976, p. 305.
[58] K.M. McCauley, J.M. Vrtis, J. Dupont, W.A. van der Donk, Insights into the functional role of the tyrosine-histidine linkage in cytochrome *c* oxidase, J. Am. Chem. Soc. 122 (2000) 2403–2404.
[59] J. Stubbe, W.A. van der Donk, Protein radicals in enzyme catalysis, Chem. Rev. 98 (1998) 705–762.
[60] Metalloenzymes involving amino acid-residue and related radicals, in: H. Sigel, A. Sigel (Eds.), Metal Ions in Biological Systems, vol. 30, Marcel Dekker, New York, 1994.
[61] T.J. Wallington, H. Egsgaard, O.J. Nielsen, J. Platz, J. Sehested, T. Stein, UV–visible spectrum of the phenyl radical and kinetics of its reaction with NO in the gas phase, Chem. Phys. Lett. 290 (1998) 363–370.
[62] J.G. Radziszewski, Electronic absorption spectrum of phenyl radical, Chem. Phys. Lett. 301 (1999) 565–570.
[63] C.L. Hawkins, M.J. Davies, Generation and propagation of radical reactions on proteins, Biochim. Biophys. Acta 1504 (2001) 196–219.
[64] F. MacMillan, A. Kannt, J. Behr, T. Prisner, H. Michel, Direct evidence for a tyrosine radical in the reaction of cytochrome *c* oxidase with hydrogen peroxide, Biochemistry-Us 38 (1999) 9179–9184.
[65] D.P. Barr, M.R. Gunther, L.J. Deterding, K.B. Tomer, R.P. Mason, ESR spin-trapping of a protein-derived tyrosyl radical from the reaction of cytochrome *c* with hydrogen peroxide, J. Biol. Chem. 271 (1996) 15498–15503.
[66] P.K. Witting, A.G. Mauk, Reaction of human myoglobin and H_2O_2—Electron transfer between tyrosine 103 phenoxyl radical and cysteine 110 yields a protein-thiyl radical, J. Biol. Chem. 276 (2001) 16540–16547.
[67] B.J. Reeder, D.A. Svistunenko, M.A. Sharpe, M.T. Wilson, Characteristics and mechanism of formation of peroxide-induced heme to protein cross-linking in myoglobin, Biochemistry-Us 41 (2002) 367–375.
[68] D.A. Svistunenko, J. Dunne, M. Fryer, P. Nicholls, B.J. Reeder, M.T. Wilson, M.G. Bigotti, F. Cutruzzola, C.E. Cooper, Comparative study of tyrosine radicals in hemoglobin and myoglobins treated with hydrogen peroxide, Biophys. J. 83 (2002) 2845–2855.
[69] M. Wikstrom, J.E. Morgan, The dioxygen cycle—spectral, kinetic, and thermodynamic characteristics of ferryl and peroxy intermediates observed by reversal of the cytochrome-oxidase reaction, J. Biol. Chem. 267 (1992) 10266–10273.
[70] W.T. Dixon, D. Murphy, Determination of the acidity constants of some phenol radical cations by means of electron spin resonance, J. Chem. Soc. Faraday Trans. 72 (1976) 1221–1230.
[71] J.P. Collman, Z. Wang, M. Zhong, L. Zeng, Syntheses and p*K*(a) determination of 1-(o-hydroxyphenyl)imidazole carboxylic esters, J. Chem. Soc. Perkin Trans. 1 8 (2000) 1217–1221.
[72] G.I. Elliott, J.P. Konopelski, Complete N-1 regiocontrol in the formation of *N*-arylimidazoles. Synthesis of the active site His-Tyr side chain coupled dipeptide of cytochrome *c* oxidase, Org. Lett. 2 (2000) 3055–3057.